

**THE GEOCHEMISTRY OF AUBRITES: INVESTIGATING REDUCED PARENT BODIES.** Z. E. Wilbur<sup>1</sup>, A. Udry<sup>2</sup>, R. A. Zeigler<sup>3</sup>, F. M. McCubbin<sup>3</sup>, K. E. Vander Kaaden<sup>1</sup>, K. Ziegler<sup>4</sup>, C. DeFelice<sup>2</sup>, and T. J. McCoy<sup>5</sup>. <sup>1</sup>Jacobs-JETS Contract, NASA Johnson Space Center, Houston, TX, USA. <sup>2</sup>University of Nevada, Las Vegas, Las Vegas, NV, USA. <sup>3</sup>NASA Johnson Space Center, Houston, TX, USA. <sup>4</sup>Institute of Meteoritics, Dept. of Earth and Planetary Sciences, University of New Mexico, Albuquerque, NM, USA. <sup>5</sup>Department of Mineral Sciences, National Museum of Natural History, Smithsonian Institution, Washington DC, USA.

**Introduction:** The aubrites (~30 known meteorites) are a unique group of differentiated meteorites that formed on asteroids with oxygen fugacities ( $fO_2$ ) from ~2 to ~6 log units below the iron-wüstite buffer [1–2]. At these highly reduced conditions, elements deviate from the geochemical behavior exhibited at terrestrial  $fO_2$ , forming FeO-poor silicates, Si-bearing metals, and exotic sulfides [3].

Here we examine the 3D mineralogy and the geochemistry of fourteen aubrites, including mineral major-element compositions, bulk-rock compositions, and oxygen isotopic compositions to understand their formation and evolution at extreme  $fO_2$  conditions. While previous studies have described the petrology and 2D modal abundances of aubrites, this work investigates the 3D modal mineralogies of silicate, metal, and sulfide phases in aubrite samples, which are then compared to the available 2D data. We utilize X-ray computed tomography (XCT) to non-destructively analyze the distribution and abundances of mineral phases in aubrites and locate composite clasts of sulfide grains for future analysis.

In order to better constrain elemental behavior under reduced conditions, we use an electron microprobe to specifically target mineral phases that comprise moderately volatile elements (i.e. oldhamite [CaS], caswellsilverite [NaCrS<sub>2</sub>], and djerfisherite [K<sub>6</sub>Na(Fe,Cu,Ni)<sub>25</sub>S<sub>26</sub>Cl]) as it has been shown that their geochemical behavior changes as a function of  $fO_2$  [3]. Understanding the behavior of moderately volatile elements has important implications for understanding reduced magmatism throughout our Solar System. This may also help us better understand the composition and mineralogy of the reduced planet Mercury [e.g. 4].

**Samples:** The following fourteen aubrites were investigated during this study: Allan Hills (ALH) 78113, ALH 84007, Bishopville, Cumberland Falls, Khor Temiki, Larkman Nunatak (LAR) 04316, LaPaz Icefield (LAP) 02233, Miller Range (MIL) 07008, MIL 13004, Mount Egerton, Northwest Africa (NWA) 8396, Norton County, Peña Blanca Spring, and Shallowater. These samples have varying degrees of brecciation and originate from two or more parent bodies [1–2]. Miller Range 07008, MIL 13004, and NWA

8396 have not been previously studied in detail aside from their initial classification.

**Methods and Results: 3D Modal Mineralogy:** The Norton County aubrite was scanned using a Nikon XTH 320 micro-XCT at NASA JSC. Scans of 8.4 and 17.9 gram samples were created with a 225 keV target reflective source using 165–185 keV. Scans were conducted with a 1 mm copper filter and have a resolution on the order of 10 s to 100 s of microns/voxels. The results of the XCT data have allowed for the determination of the abundances of silicate groundmass (i.e., enstatite, forsterite, albite, and diopside), light (based on electron density) sulfides (i.e., alabandite [MnS] and daubréelite [FeCr<sub>2</sub>S<sub>4</sub>]), heavy (based on electron density) sulfides (i.e., troilite [FeS]), and Fe,Ni metal by segmenting a density histogram in *Volume Graphics Studio* software. The discernable phases are within ~5% of the linear attenuation coefficients (LAC) [5]. The modal results of the scans are: 96.9 vol.% silicates and groundmass, 0.8 vol.% light sulfides, 1.5 vol.% heavy sulfides, and 0.9 vol.% metal. Our 2D modal abundances of Norton County are: 98.8 vol.% silicates and groundmass, 1.2 vol.% sulfides, and 1.2 vol.% metal. These 2D modal results were determined using *Image J* software, which has an error of ~5% [6]. XCT scans of additional aubrites are underway.

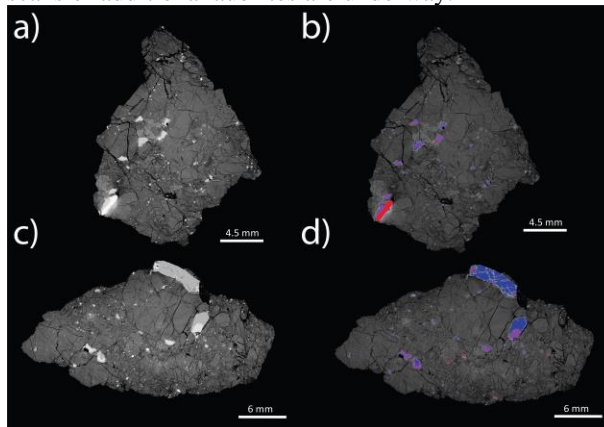


**Figure 1:** XCT scans of Norton County, a) and c) are scans where changes in brightness are proportional to differences in linear attenuation coefficients, or LAC (a measure of a mineral's density and composition); b) and d) are scans with phases isolated using *Volume*

Graphics Studio software. Light sulfides are in blue, heavy sulfides are in purple, and metals are in red.

**Bulk Rock Geochemistry:** Aubrite bulk rock geochemical compositions were measured using inductively coupled mass spectrometry (ICP-MS) at the University of Nevada, Las Vegas. The aubrites have higher abundances of rare Earth elements (REE) in this study compared to aubrites analyzed in [7]. This enrichment may be an artifact of the amount of sulfides dissolved for analysis. It has been shown that oldhamite (CaS) is the major REE carrying phase in aubrites [8]. A greater amount of oldhamite present in the heterogeneous aliquots for dissolution may be attributed to the enriched aubrite patterns.

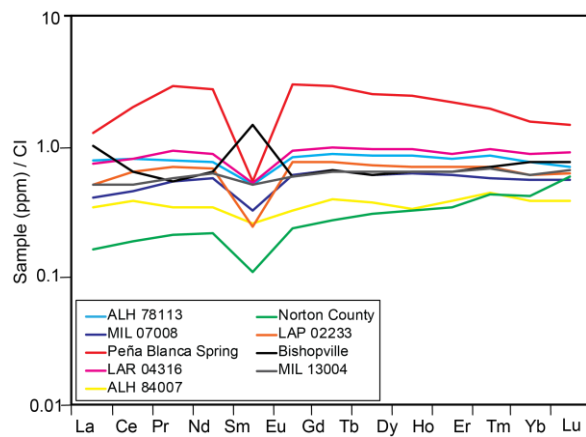


Figure 2: Rare earth element patterns of the studied aubrites. The heterogeneous nature of the aubrites is reflected in their bulk rock patterns. It should be noted that there is a possibility of cryptic plagioclase fractionation.

**Oxygen Isotopic Compositions:** Oxygen isotopic compositions were analyzed at the University New Mexico. Samples were initially treated to remove terrestrial alteration. The aubrite oxygen isotopic compositions in this study (Figure 3) show more heterogeneity compared to aubrites in previous studies [7,9]. This heterogeneity could reflect that the aubrite parent bodies are isotopically heterogeneous and may have undergone incomplete differentiation.

**Discussion:** We aim to better understand reduced elemental partitioning, as this has important implications for understanding reduced magmatism on other bodies in our Solar System, such as Mercury [4]. The 3D modal mineralogical results in this study give similar volume percentages as 2D modal results. We have located composite clasts of metal and sulfide grains for future analytical study. The use of XCT is a powerful tool to nondestructively observe the internal composi-

tion of precious meteoritic material. The high resolution detector, multiple sources, and large stage in the Nikon XTH 320 micro-XCT machine offer the flexibility to analyze a wide range of future aubrite sample sizes [10].

**Moderately Volatile Element Partitioning in Reduced Bodies:** The geochemical behavior of moderately volatile elements changes as a function of  $fO_2$  [3]. Bulk distribution coefficient calculations are underway for the studied aubrites. We use the formula  $D_i = c_i^X / c_i^Y$ , where  $c$  is the concentration of element  $i$  in phase  $X$  and  $Y$  (metal, sulfide, or silicate), and include modal abundances of silicate, sulfide, and metal phases and mineral major element data. Moderately volatile elements are present in reduced bodies, including Mercury [11–12], which was not expected due to their close proximity to the Sun. Constraining their partitioning at low  $fO_2$  can provide insight into the distribution and magmatic evolution on reduced differentiated bodies.

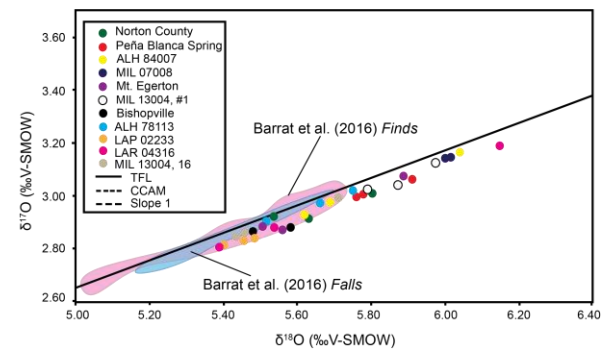


Figure 3: Oxygen isotopic compositions,  $\delta^{18}O$  versus  $\delta^{17}O$  of studied aubrites, including fields of aubrite finds and falls from [7]. The aubrite finds in this study contrast most with the aubrite finds from [7]. Samples in this study plot below the TFL and exhibit more heterogeneous linearized  $\Delta^{17}O$  patterns (which represents a linear deviation from the TFL). Errors are smaller than the symbols.

**References:** [1] Keil K. (1968) *JGR*, 73, 6945–6976. [2] Keil K. (2010) *Chemie de Erde*, 70, 295–317. [3] Kaufman S. V. (2016) *LPS XXVII*, Abstract #2743. [4] McCoy T. J. and Bullock E. S. (2017) *Planetesimals*, 71–91. [5] Tsuchiyama A. et al. (2005) *Am. Min.*, 90, 132–142. [6] Maloy A. K. and Treiman A. H. (2007) *Am. Min.*, 92, 1781–1788. [7] Barrat J. A. (2016) *GCA*, 192, 29–48. [8] Wheelock M. M. et al. (1994) *GCA*, 58, 449–458. [9] Clayton R. N. and Mayeda T. K. (1996) *GCA* 60, 1999–2017. [10] Zeigler R. A. et al. (2018) *LPS XXVII*, Abstract #6061. [11] McCoy T. J. et al (1999) *Meteoritics and Planetary Science*, 34, 735–746. [12] Vander Kaaden K. E. and McCubbin F. M. (2016) *GCA*, 173, 246–263.